

NACA RM L56F19a

GPO PRICE \$

CFSTI PRICE(S) \$

Hard copy (HC) 2.00

Microfiche (MF) 1.50

ff 653 July 65

NACA

Declassified by authority of NASA
Classification Change Notice No. 26-111
Dated 00 7/20/66

X62-63951
Copy 339
RM L56F19a

RESEARCH MEMORANDUM

LOW-SPEED INVESTIGATION OF THE EFFECT OF SMALL CANARD
SURFACES ON THE DIRECTIONAL STABILITY OF A
SWEPTBACK-WING FIGHTER-AIRPLANE MODEL

By John W. Paulson and Peter C. Boisseau

Langley Aeronautical Laboratory
Langley Field, Va.

DECLASSIFIED- AUTHORITY
CS 1351 DRUMMA TO 1351
MEMO DATED 6/10/65

N66 34101

(ACCESSION NUMBER)

26

(PAGES)

(NASA CR OR TMX OR AD NUMBER)

(THRU)

1

(CODE)

02

(CATEGORY)

NATIONAL ADVISORY COMMITTEE
FOR AERONAUTICS

WASHINGTON

August 23, 1956

NATIONAL ADVISORY COMMITTEE FOR AERONAUTICS

RESEARCH MEMORANDUM

LOW-SPEED INVESTIGATION OF THE EFFECT OF SMALL CANARD
SURFACES ON THE DIRECTIONAL STABILITY OF A
SWEEPBACK-WING FIGHTER-AIRPLANE MODEL

By John W. Paulson and Peter C. Boisseau

SUMMARY

N66 34181

A low-speed investigation has been made in the Langley free-flight tunnel to determine the effect of small canard surfaces on the directional stability of a fighter-airplane model having an aspect ratio of 3.4 and a 42° sweptback wing. The canard surfaces were found to be generally ineffective at angles of attack below 20° . For higher angles of attack, small canard surfaces ($4\frac{1}{2}$ by 27 inches, full scale) reduced the directional instability of the model at low angles of sideslip ($\beta < 5^\circ$) but provided no improvement at higher angles of sideslip. These canard surfaces had virtually no effect on the longitudinal characteristics.

A-16 601

INTRODUCTION

Recent tests of a sweptback-wing fighter-airplane model in the Langley 20-foot free-spinning tunnel (ref. 1) showed that the spin recovery characteristics were improved through the use of canard surfaces, some of which represented open electrical access doors. Additional tests on a catapult facility showed that the canard surfaces, when located at certain positions, also had a favorable effect on the directional stability characteristics of the model at high angles of attack.

Since the canard surfaces used in the tests of reference 1 were rather large and probably caused undesirably large reductions in longitudinal stability, force tests were made in the Langley free-flight tunnel of a generally similar model with smaller, lower-aspect-ratio surfaces to see if such surfaces might still produce the favorable directional stability effects without the detrimental longitudinal effects. Surfaces such as these might be small enough to be permanently installed on the nose of the ~~model~~ ~~are~~ ~~installed~~ on a wing.

The tests were made as part of an investigation being conducted by the Langley free-flight tunnel section to determine the dynamic stability and control characteristics of a general research airplane model similar to current fighter designs. Tests were made with the simulated access doors and with the various sizes and shapes of canard surfaces located at different longitudinal and vertical positions on the forward part of the fuselage. For comparison purposes, tests were made with large canard surfaces which were assumed to simulate open electrical access doors.

SYMBOLS

The data are referred, in all cases, to the stability system of axes shown in figure 1. The coefficients are based on the dimensions of the wing plan form which neglect the chord-extension. The center of gravity was located at 28.7 percent of the mean aerodynamic chord.

b wing span, ft

C_D drag coefficient, Drag/qS

C_L lift coefficient, Lift/qS

C_l rolling-moment coefficient, M_X/qSb

$$C_{l_\beta} = \frac{\partial C_l}{\partial \beta}$$

C_m pitching-moment coefficient, $M_Y/qS\bar{c}$

C_n yawing-moment coefficient, M_Z/qSb

$$C_{n_\beta} = \frac{\partial C_n}{\partial \beta}$$

C_Y lateral-force coefficient, F_Y/qS

$$C_{Y_\beta} = \frac{\partial C_Y}{\partial \beta}$$

\bar{c} mean aerodynamic chord, ft


F_D	drag force, lb
F_L	lift force, lb
F_Y	lateral force, lb
M_X	rolling moment, ft-lb
M_Y	pitching moment, ft-lb
M_Z	yawing moment, ft-lb
q	dynamic pressure, lb/sq ft
S	area, sq ft
V	airspeed, ft/sec
α	angle of attack of fuselage reference line, deg
β	angle of sideslip, deg
ρ	air density, slugs/cu ft
ϕ	angle of roll, deg
ψ	angle of yaw, deg

Subscripts:

vt	vertical tail
w	wing

APPARATUS AND MODEL

The model was tested in the Langley free-flight tunnel, which is a low-speed tunnel with a 12-foot octagonal test section. A sting-type support system and an internally mounted three-component strain-gage balance were used.





A three-view drawing of the model used in the investigation is presented in figure 2, and the dimensional characteristics are given in table I. Presented in table II are sketches showing the canard surfaces tested.

TESTS


Force tests were made in order that the effect of the various canard surfaces on the lateral stability characteristics of the model up to an angle of attack of 50° could be studied. The exploratory runs were generally made over a sideslip range of $\pm 10^\circ$, and then some of the more promising configurations were tested over a range of $\pm 20^\circ$ with vertical tail off and on. The tests were made with all controls set at a deflection of 0° , with a wing incidence of -1° , and with an incidence of 0° of the canard surfaces.

All tests were run at a dynamic pressure of 4.3 pounds per square foot which corresponds to an airspeed of approximately 61 feet per second at standard sea-level conditions and to a test Reynolds number of 511,000 based on the mean aerodynamic chord of 1.309 feet.

RESULTS AND DISCUSSION

Lateral Stability Characteristics

Basic model and model with access doors extended.— The variation of the coefficients C_Y , C_n , and C_l with sideslip angle for various angles of attack is shown in figures 3 and 4 for the basic model and for the model with access doors extended, respectively. The data for the model with vertical tail off (fig. 3(a)) show that the model was directionally unstable throughout the angle-of-attack range. The yawing-moment coefficient varied linearly with the angle of sideslip and indicated about the same degree of directional instability for the model at all angles of attack except at 50° , where the model was less unstable at small angles of sideslip than it was at the higher angles. With the vertical tail on (fig. 3(b)), the model was directionally stable for moderate angles of sideslip up to an angle of attack of about 17° or 18° , and the variation of C_n with the angle of sideslip was nonlinear for most angles of attack. The data of figure 4 show that the extended access doors resulted in the model's being directionally stable for small angles of sideslip at angles of attack above 25° with vertical tail off or on. At the larger sideslip angles, however, the model was still directionally unstable. Since the access doors improved the directional stability of the model with vertical tail off or on, their effect was apparently






achieved by changing the flow over the fuselage and the wing. A direct comparison of some of the data of figures 3 and 4 is made in figure 5. This figure shows that there is virtually no effect of the access doors on the directional stability of the model at an angle of attack of 20° but that there is a large stabilizing effect at small angles of sideslip for an angle of attack of 30° . A further comparison of the data of figures 3 and 4 is made in figure 6 where the variation with angle of attack of the stability derivatives C_{n_β} and C_{l_β} , as measured at various sideslip angles, are presented. These data show that the access doors had the greatest effect on the directional stability at angles of attack above 20° and at low angles of sideslip. These results are in fair agreement with those presented in reference 1.

Effect of canard size and shape.- Since the preliminary force tests showed that the extended access doors produced some favorable effects on the directional stability characteristics, additional tests were made with canard surfaces of different sizes (see table II) in an effort to find a small canard surface that would produce essentially the same characteristics as the access doors. Presented in figure 7 are the data from these tests compared with those for the basic model and for the access doors extended. The data show that none of the canards had any significant effect on the directional stability at an angle of attack of 20° . At an angle of attack of 30° , however, stabilizing effects comparable to those of the access doors were obtained at small angles of sideslip for canard surfaces as small as $1/2$ by 3 inches.

Effect of canard position and size.- In order to determine the effect of canard position on the directional stability characteristics, force tests were made in which canard surfaces of different sizes were located at various positions on the fuselage as shown in table II. The tests were made at angles of attack of 20° and 30° , and the data are summarized in figure 8. The data again show that, at an angle of attack of 20° , none of the canard positions or sizes had any significant effect on the directional stability characteristics. At an angle of attack of 30° , however, stabilizing effects were obtained at a number of positions, and the greatest effects occurred at positions 1, 2, 7, 8, or 13. The most favorable position appeared to be position 2, and data obtained from tests made to determine the variation of the lateral coefficients over a sideslip range of $\pm 20^\circ$ for the $1/2$ - by 3-inch canard surface at this position are presented in figure 9.

Comparison of access door and $1/2$ - by 3-inch canard effects.- Summarized in figure 10 are the lateral stability derivatives C_{Y_β} , C_{n_β} , and C_{l_β} measured at angles of sideslip of $\pm 5^\circ$ and $\pm 20^\circ$ for the basic model, for the model with the access doors, and for the model with the $1/2$ - by 3-inch canard surfaces. The figure shows that the canard





surfaces were generally ineffective at angles of attack below 20° . For higher angles of attack, both the access doors and the 1/2- by 3-inch canard surfaces reduced the directional instability of the model at low angles of sideslip ($\beta < 5^\circ$) but provided little or no improvement at higher angles of sideslip. The variation of the effective dihedral parameter C_{l_β} with angle of attack was generally similar for all cases except the access doors at sideslip angles of $\pm 5^\circ$.

Longitudinal Characteristics

A comparison is made in figure 11 of the longitudinal characteristics of the model in its basic configuration, with access doors extended, and with the 1/2- by 3-inch canard surfaces. The data show that the access doors contributed a small lift increment near the stall but reduced the longitudinal stability over the entire angle-of-attack range. The small canard surface, however, did not have any significant effect on the longitudinal characteristics.

CONCLUDING REMARKS

A low-speed investigation conducted in the Langley free-flight tunnel to determine the effect of small canard surfaces on the directional stability of a fighter-airplane model showed that these surfaces were generally ineffective at angles of attack below 20° . For higher angles of attack, small canard surfaces ($4\frac{1}{2}$ by 27 inches, full scale) reduced the directional instability of the model at low angles of sideslip ($\beta < 5^\circ$) but provided no improvement at higher angles of sideslip. The canard surfaces also had virtually no effect on the longitudinal characteristics.

Langley Aeronautical Laboratory,
National Advisory Committee for Aeronautics,
Langley Field, Va., June 5, 1956.



REFERENCE

1. Klinar, Walter J.: A Study by Means of a Dynamic-Model Investigation of the Use of Canard Surfaces as an Aid in Recovering From Spins and As a Means for Preventing Directional Divergence Near the Stall. NACA RM L56B23, 1956.



TABLE I.- DIMENSIONAL CHARACTERISTICS OF MODEL TESTED
IN LANGLEY FREE-FLIGHT TUNNEL

Wing:

Airfoil section at root	NACA 65A006
Airfoil section at tip	NACA 65A005
Area, sq ft	4.63
Span, ft	3.96
Aspect ratio	3.39
Root chord (on fuselage reference line), ft	1.87
Tip chord (without chord-extension), ft	0.462
Tip chord (with chord-extension), ft	0.518
Mean aerodynamic chord, \bar{c} , ft	1.306
Sweep of quarter-chord line, deg	42
Dihedral, deg	-5
Taper ratio (without chord-extension)	0.247
Incidence, deg	-1

Horizontal tail:

Airfoil section at root	NACA 65A006
Airfoil section at tip	NACA 65A004
Area (total), sq ft	1.154
Span, ft	2.01
Root chord (on fuselage reference line), ft	1.00
Tip chord, ft	0.148
Sweep of quarter-chord line, deg	45
Dihedral, deg	5.42
Aspect ratio	3.50
Taper ratio	0.148

Vertical tail:

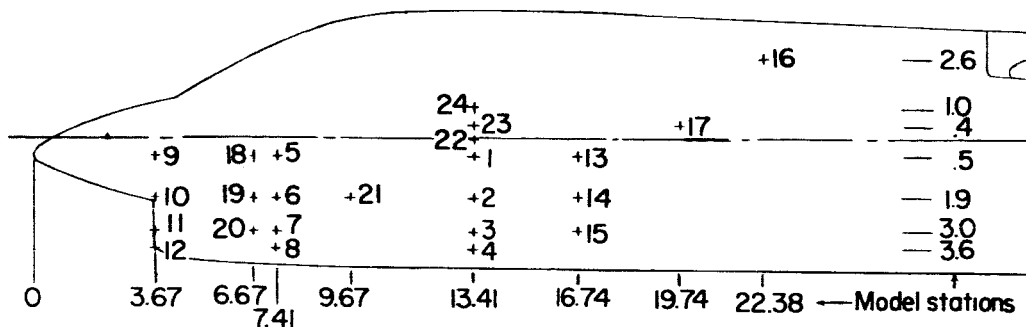
Airfoil section at root	NACA 65A006
Airfoil section at tip	NACA 65A004
Area (including 0.0926 sq ft of exposed dorsal fin), sq ft	1.0
Span (measured from fuselage reference line), ft	1.343
Root chord (on fuselage reference line), ft	1.455
Tip chord, ft	0.380
Sweep of quarter-chord line, deg	45
Area ratio, S_{vt}/S_w , percent	21.6
Aspect ratio	1.802
Taper ratio	0.26

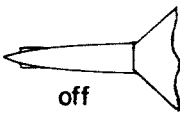
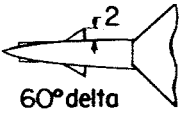
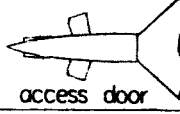
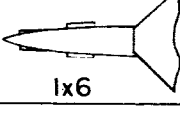
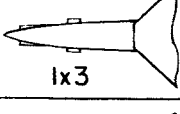
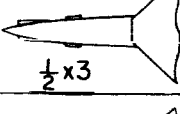
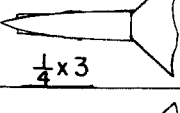
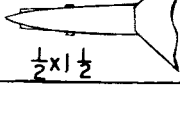


~~SECRET~~

TABLE II.- SUMMARY OF CANARD POSITIONS TESTED

[Crosses indicate location of canard leading edge. Canard was perpendicular to local fuselage surface.]



Canard surfaces	Positions tested	Angle of attack	Sideslip range
 off	—	0 to 50	± 20
 60° delta	2	20, 30	± 10
 access door	1	15 to 50	± 20
 1x6	1 thru 16 2, 7, 11, 16	30 20	± 10 ± 10
 1x3	1, 2, 10, 11, 13, 17, 18, 19, 20, 21 1, 2, 10, 13, 17, 18	20 30	± 10 ± 10
 $\frac{1}{2} \times 3$	2 22, 23, 24	15 to 30 15 to 40 20, 30	± 10 ± 20 ± 10
 $\frac{1}{4} \times 3$	2	30	± 10
 $\frac{1}{2} \times 1 \frac{1}{2}$	2	20, 30	± 10

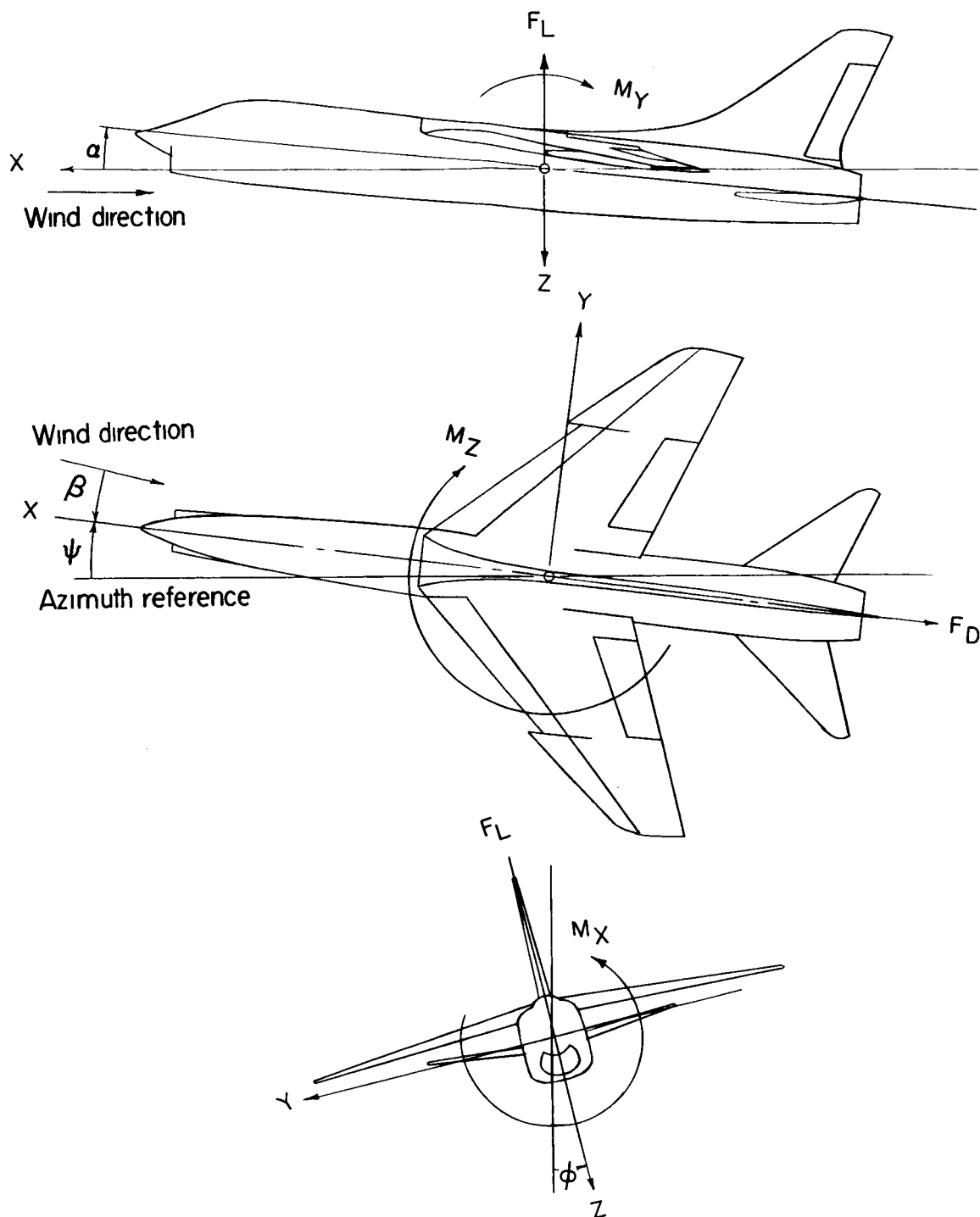


Figure 1.- The stability system of axes. Arrows indicate the positive direction of forces, moments, and angular displacements.

[REDACTED]

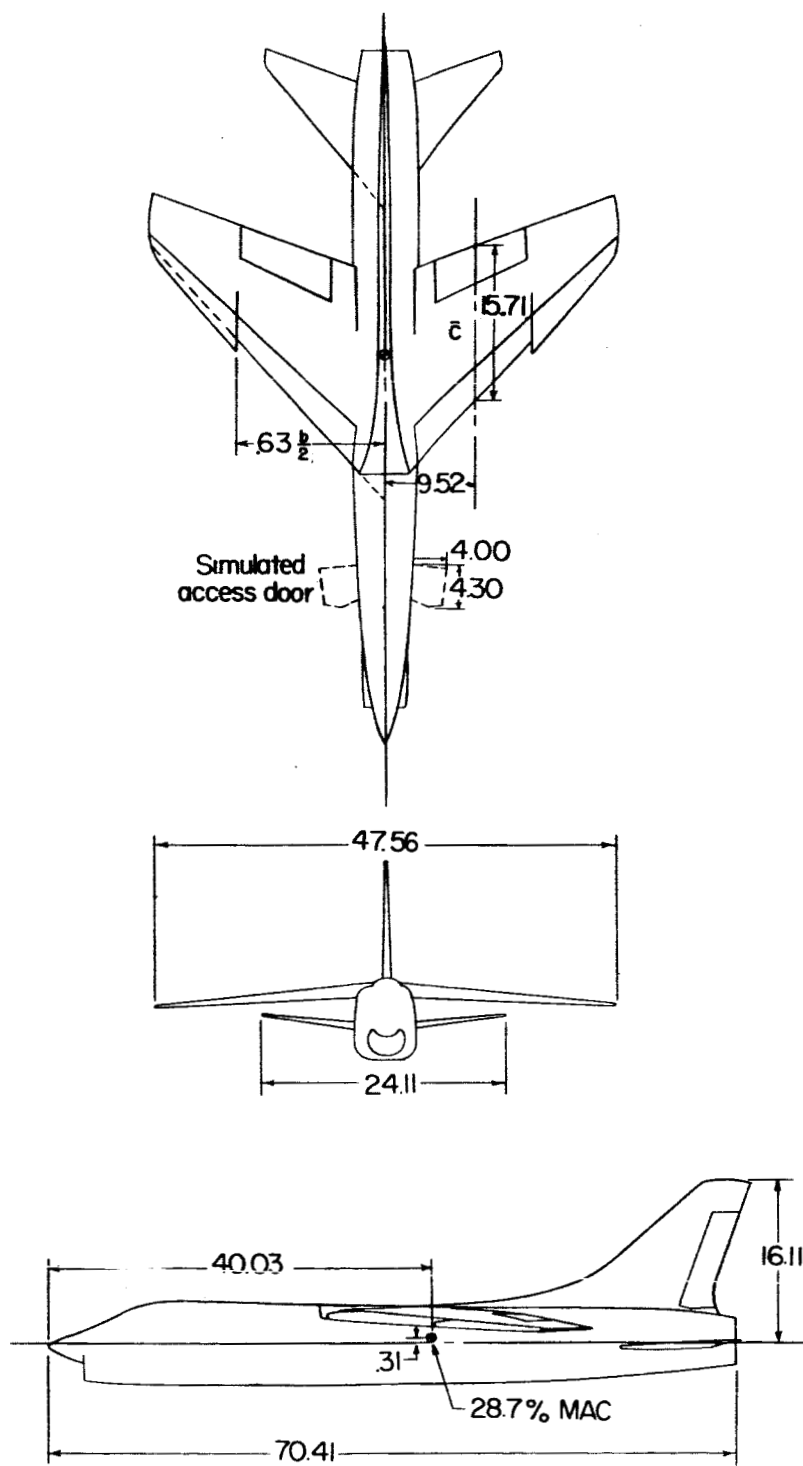
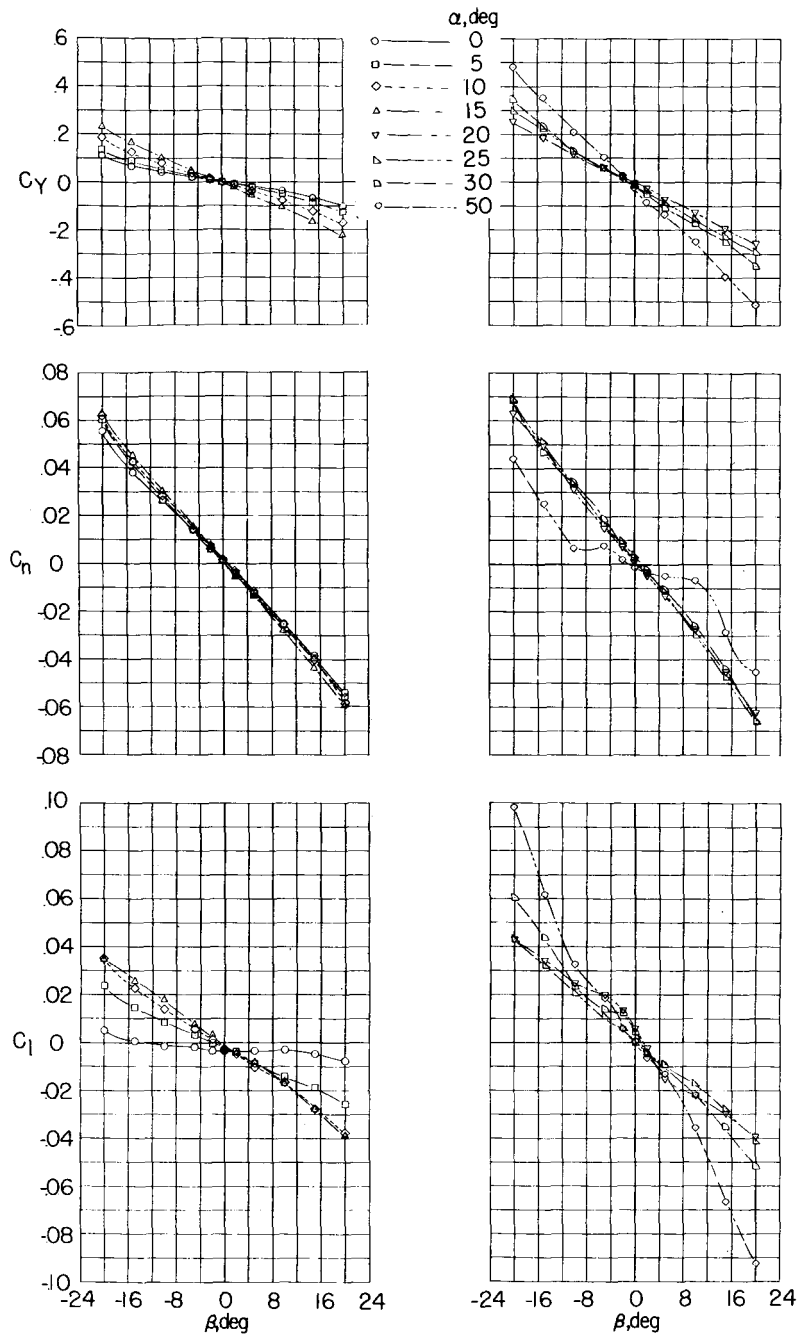
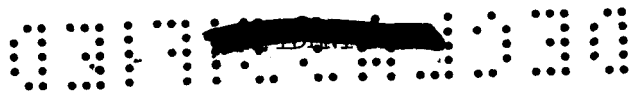


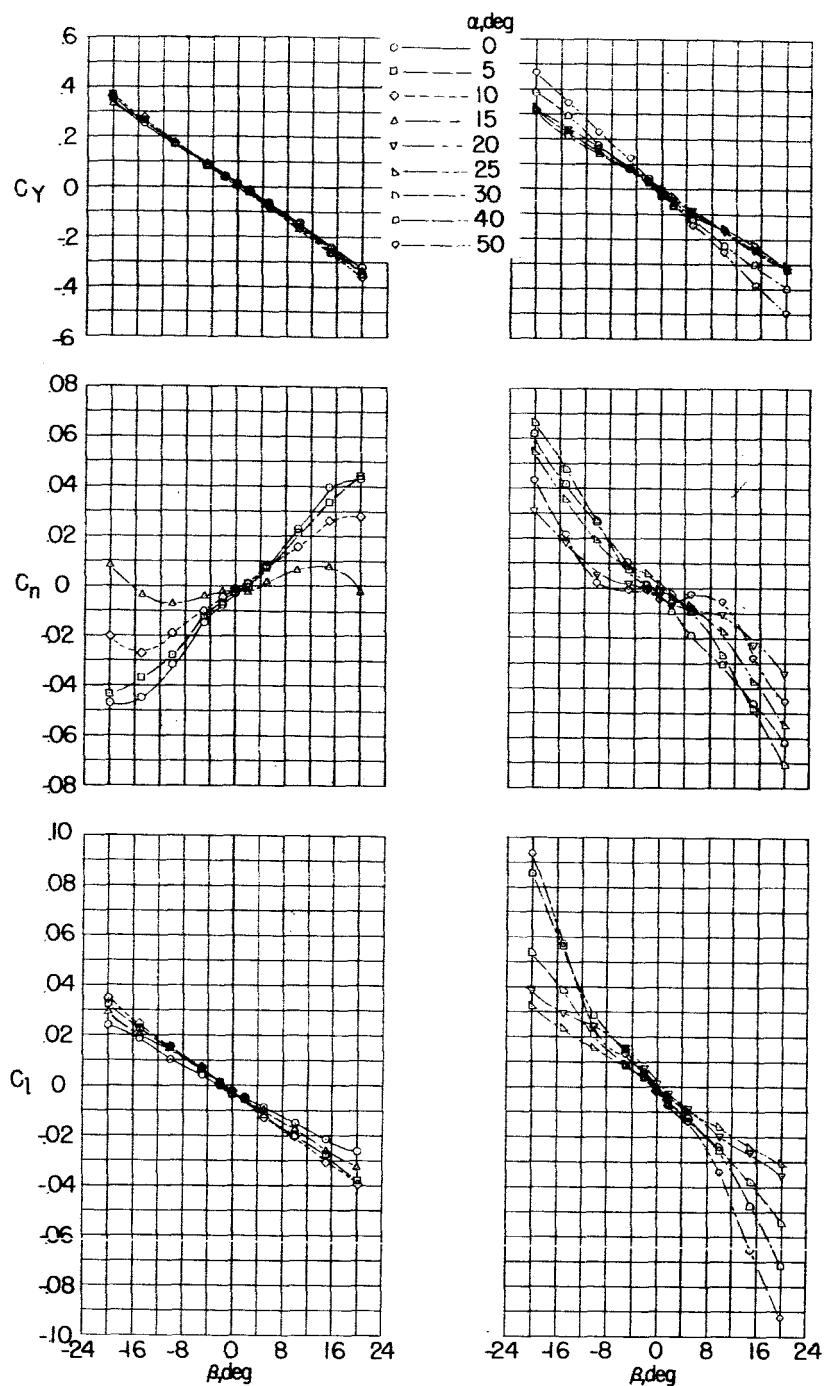
Figure 2.- Sketch of model used in investigation. All dimensions are in inches.



(a) Tail off.

Figure 3.- Variation of the static lateral stability characteristics with angle of sideslip. Basic configuration.





(b) Tail on.

Figure 3.- Concluded.

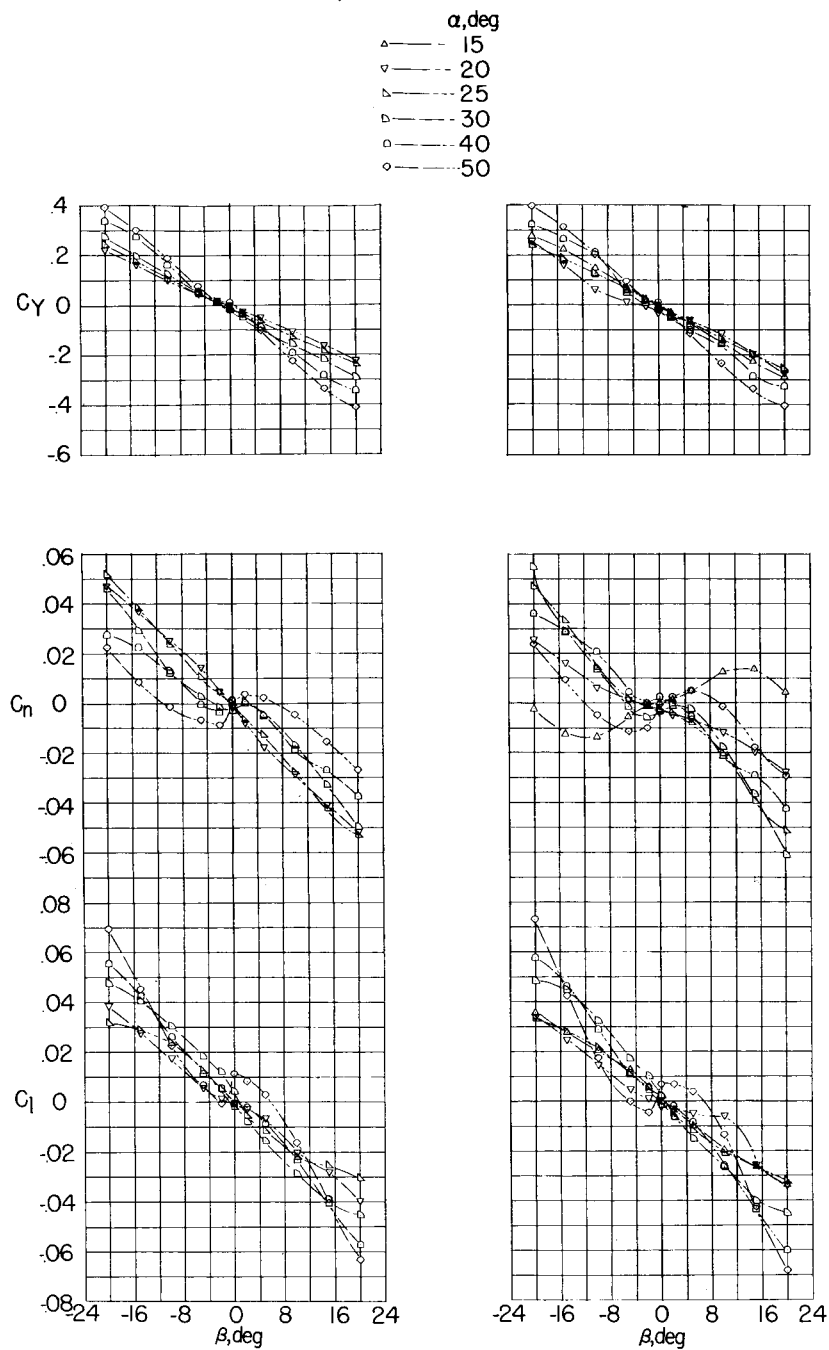


Figure 4.- Variation of static lateral stability characteristics with angle of sideslip. Access doors extended.



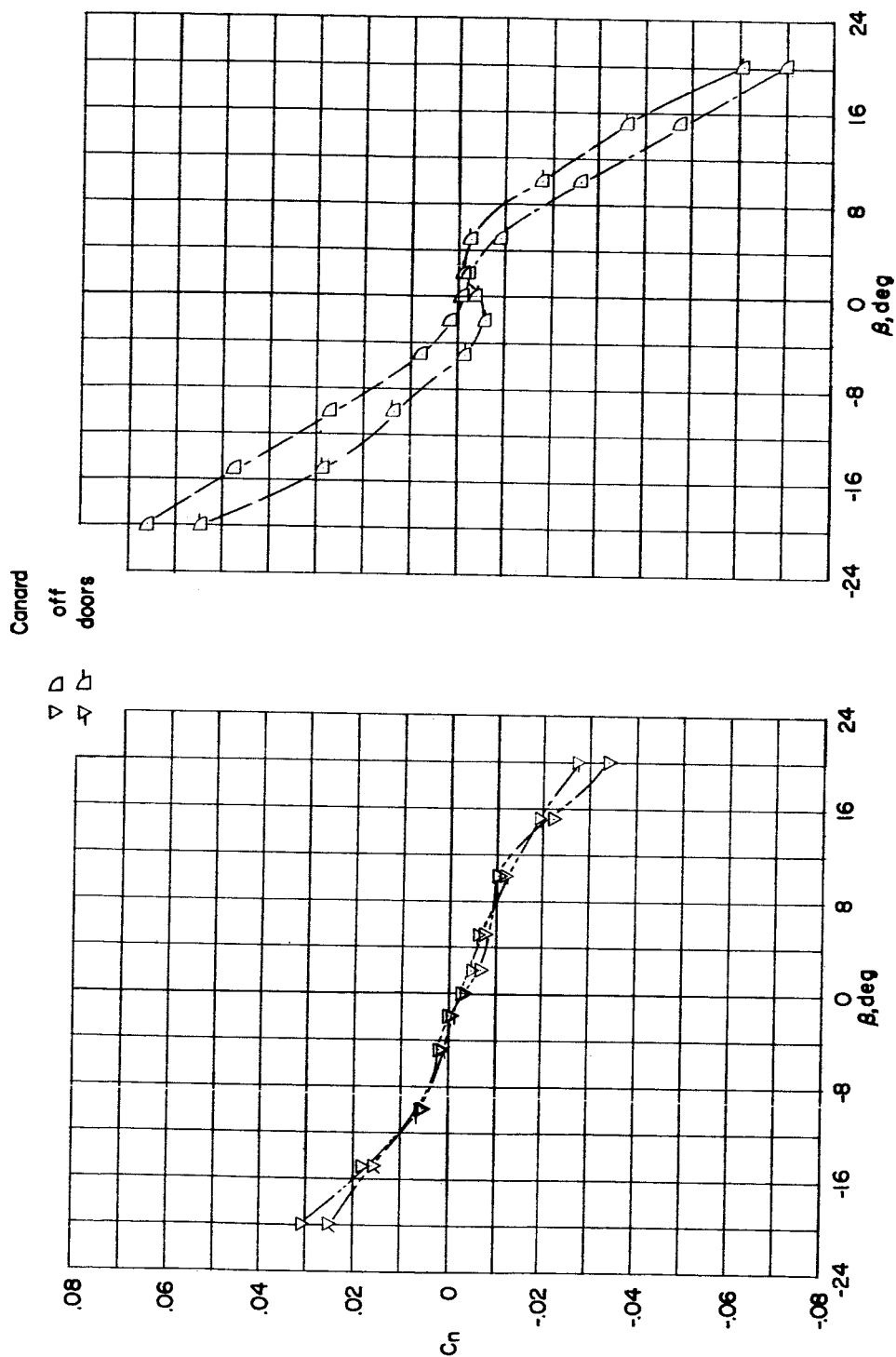


Figure 5.- Effect of access doors on variation of yawing-moment coefficient with angle of sideslip.

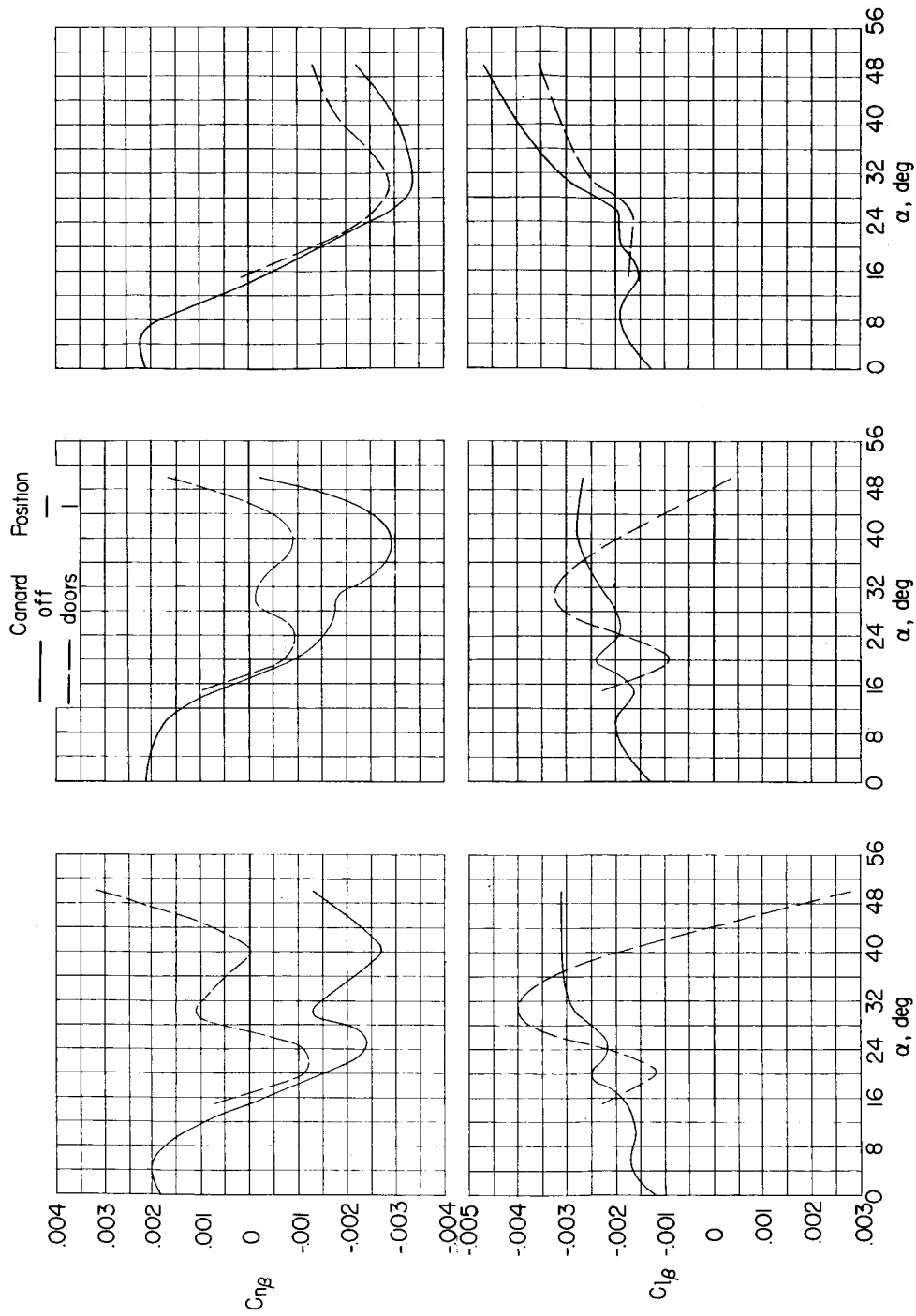
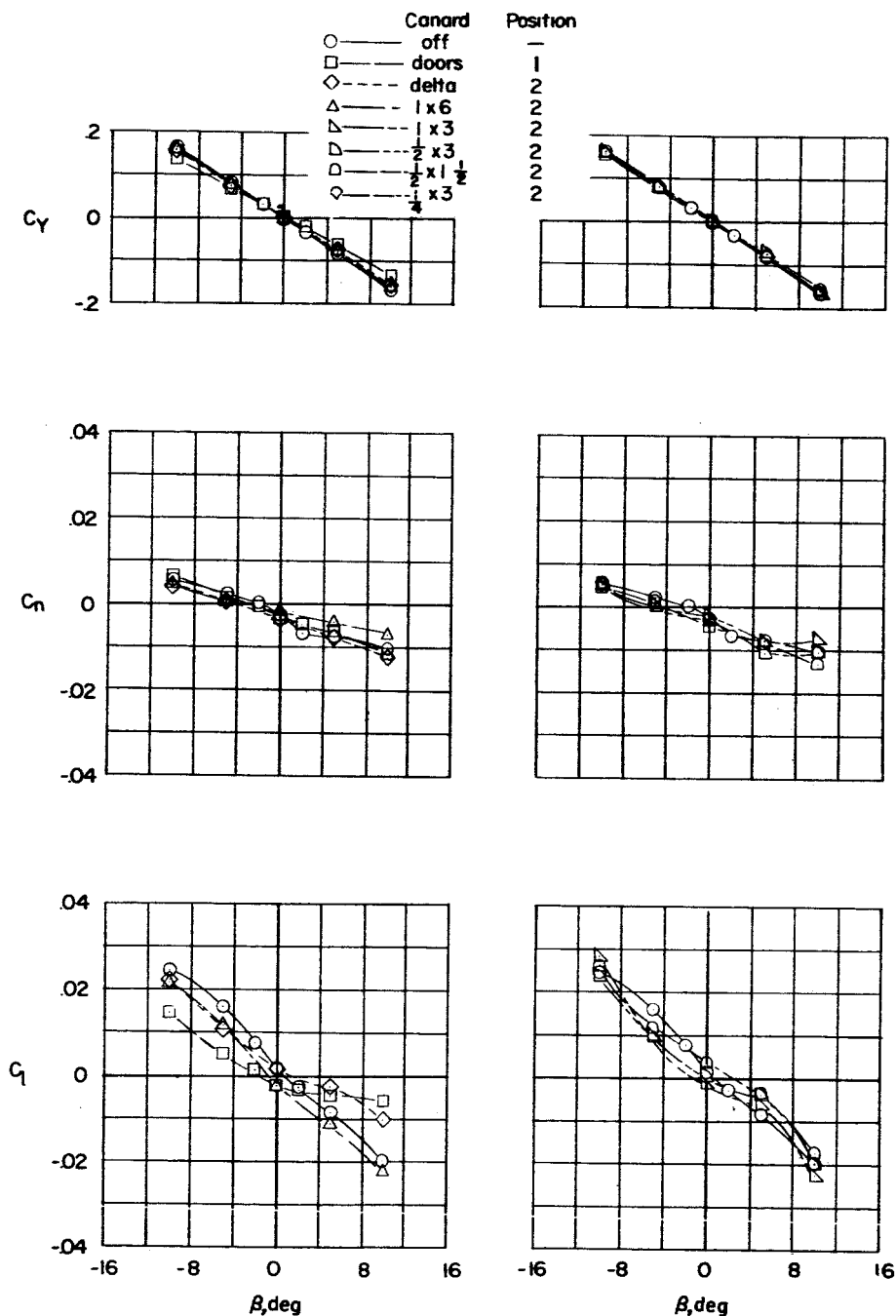
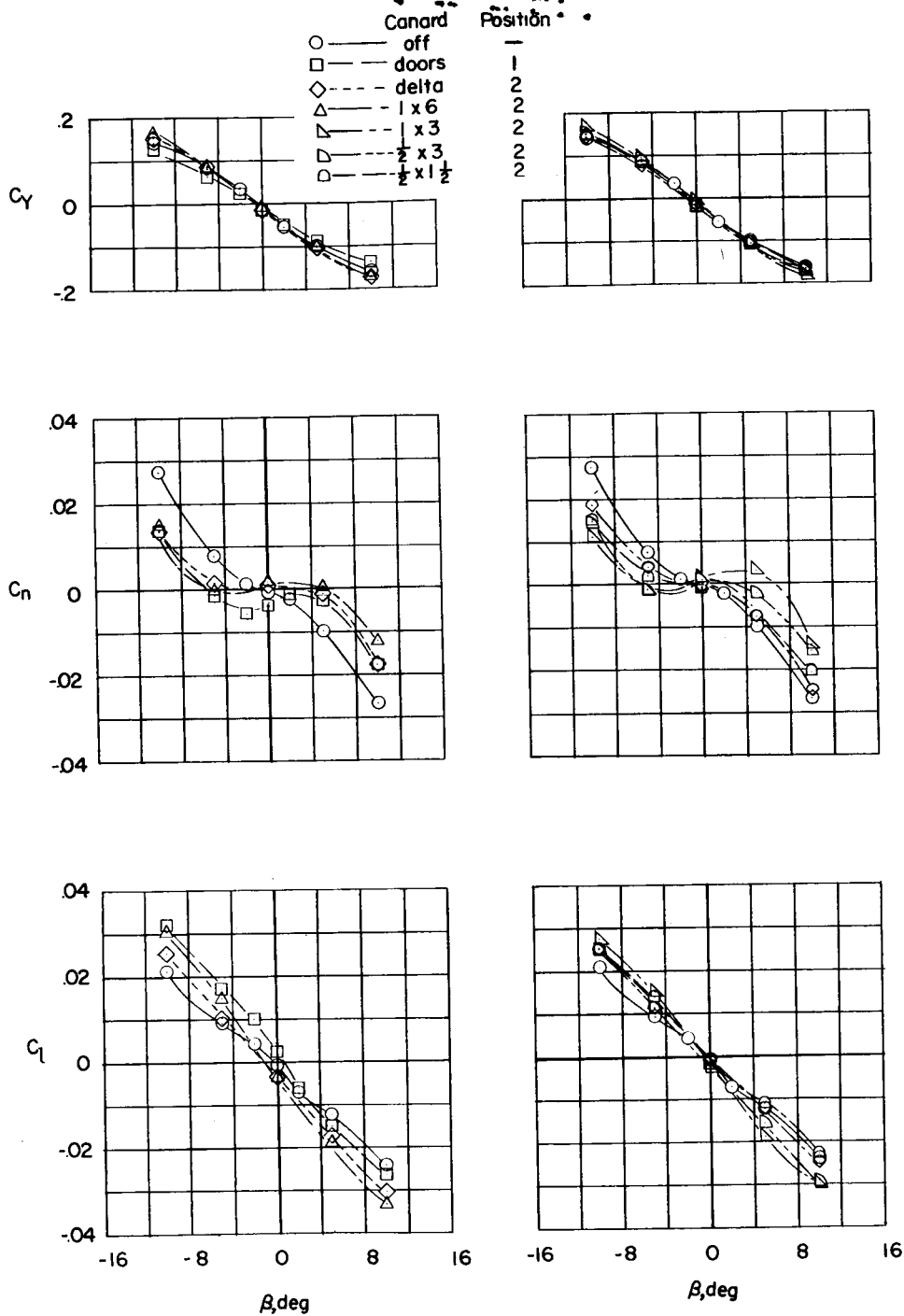
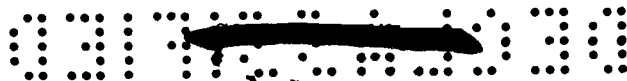


Figure 6.- Effect of canard surfaces on the variation of static sideslip derivatives with angle of attack. Tail on.



(a) $\alpha = 20^\circ$.

Figure 7.- Effect of canard size and shape on the variation of static lateral stability characteristics with angle of sideslip. Tail on. All dimensions are in inches.



(b) $\alpha = 30^\circ$.

Figure 7.- Concluded.



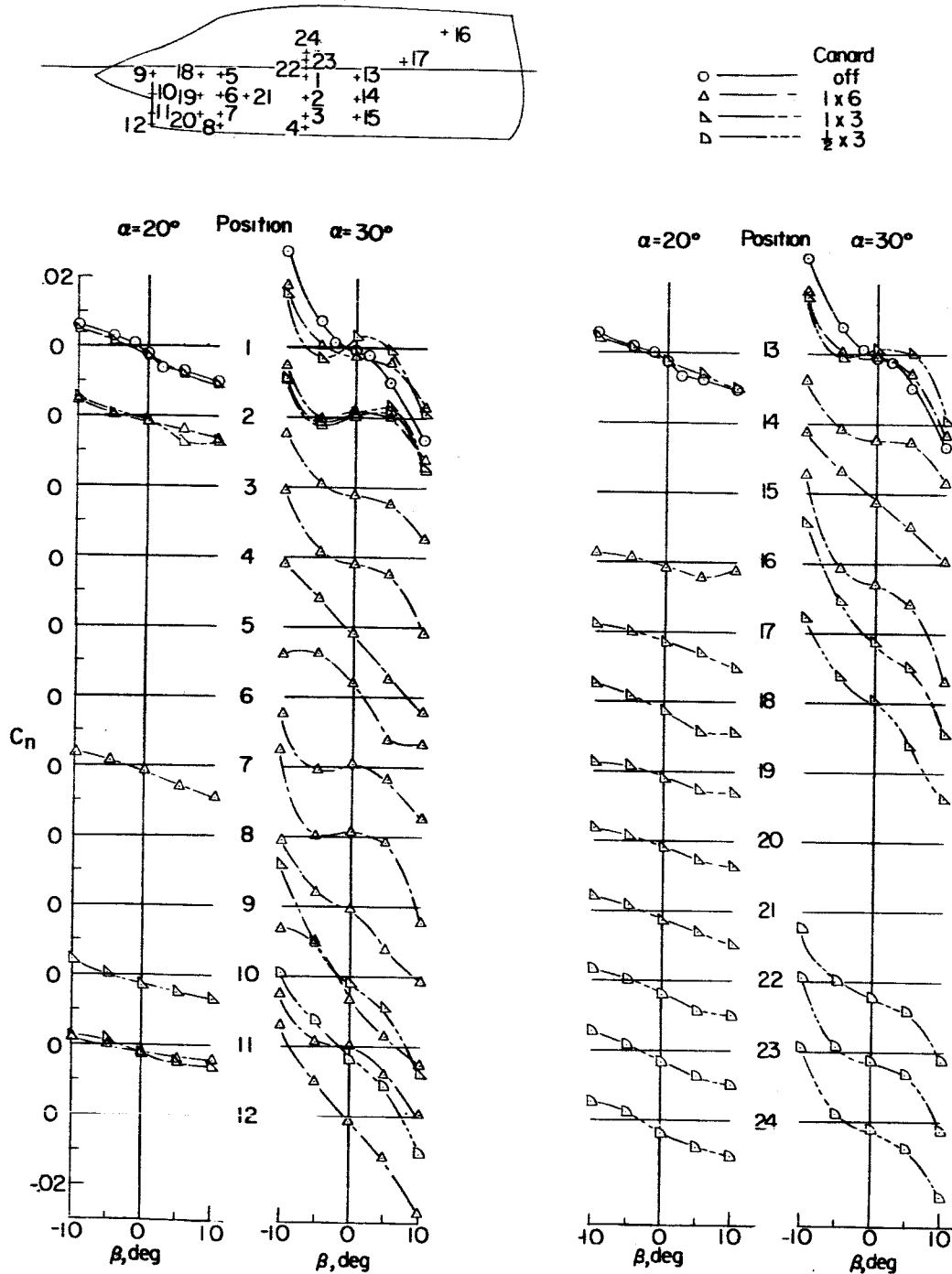
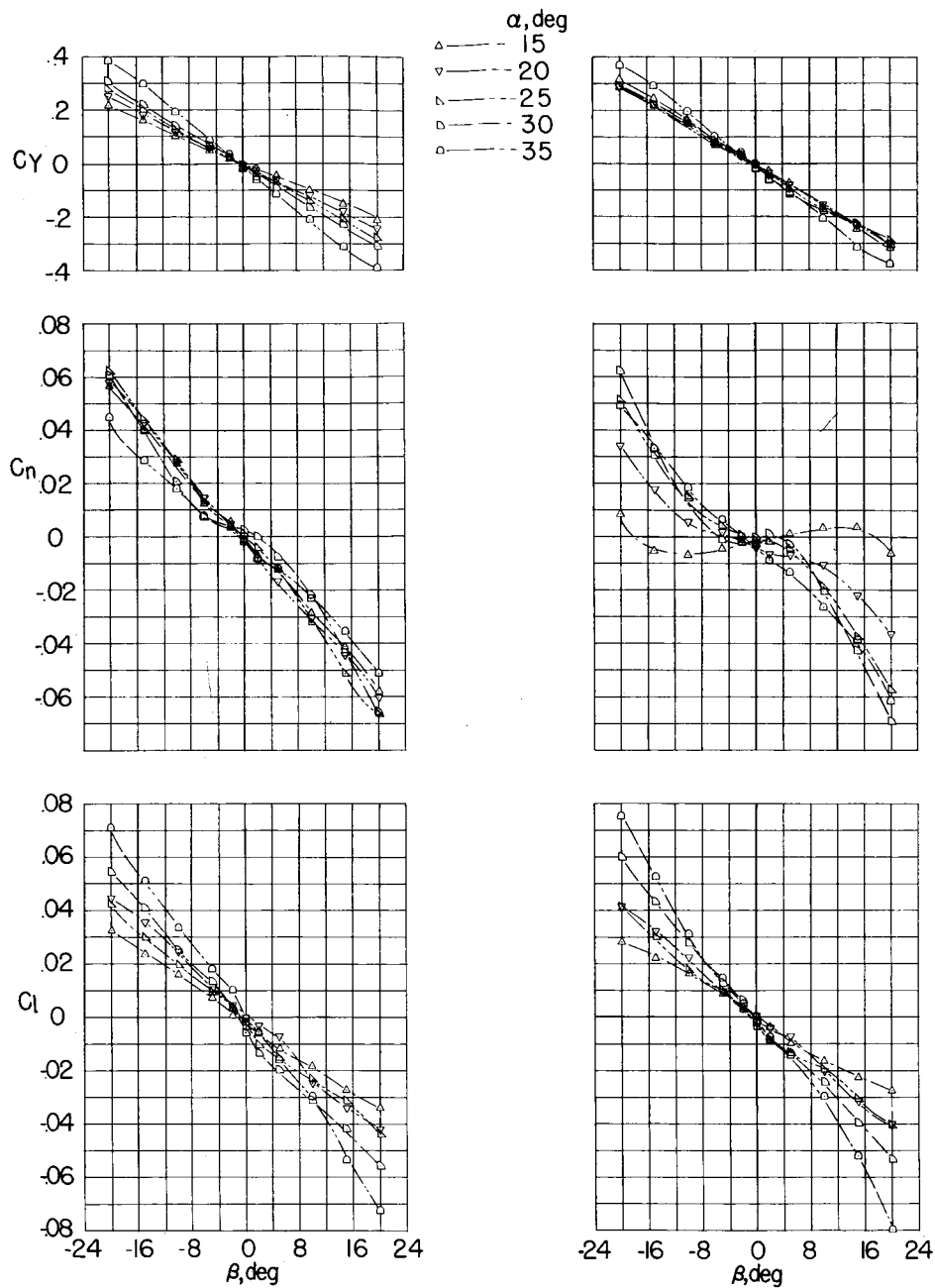


Figure 8.- Effect of canard position and size on the variation of static lateral stability characteristics with angle of sideslip. Tail on. All dimensions are in inches.



(a) Tail off.

(b) Tail on.

Figure 9.- Effect of angle of attack on variation of the static lateral stability characteristics with angle of sideslip for the $\frac{1}{2}$ - by 3-inch canard surface at position 2.

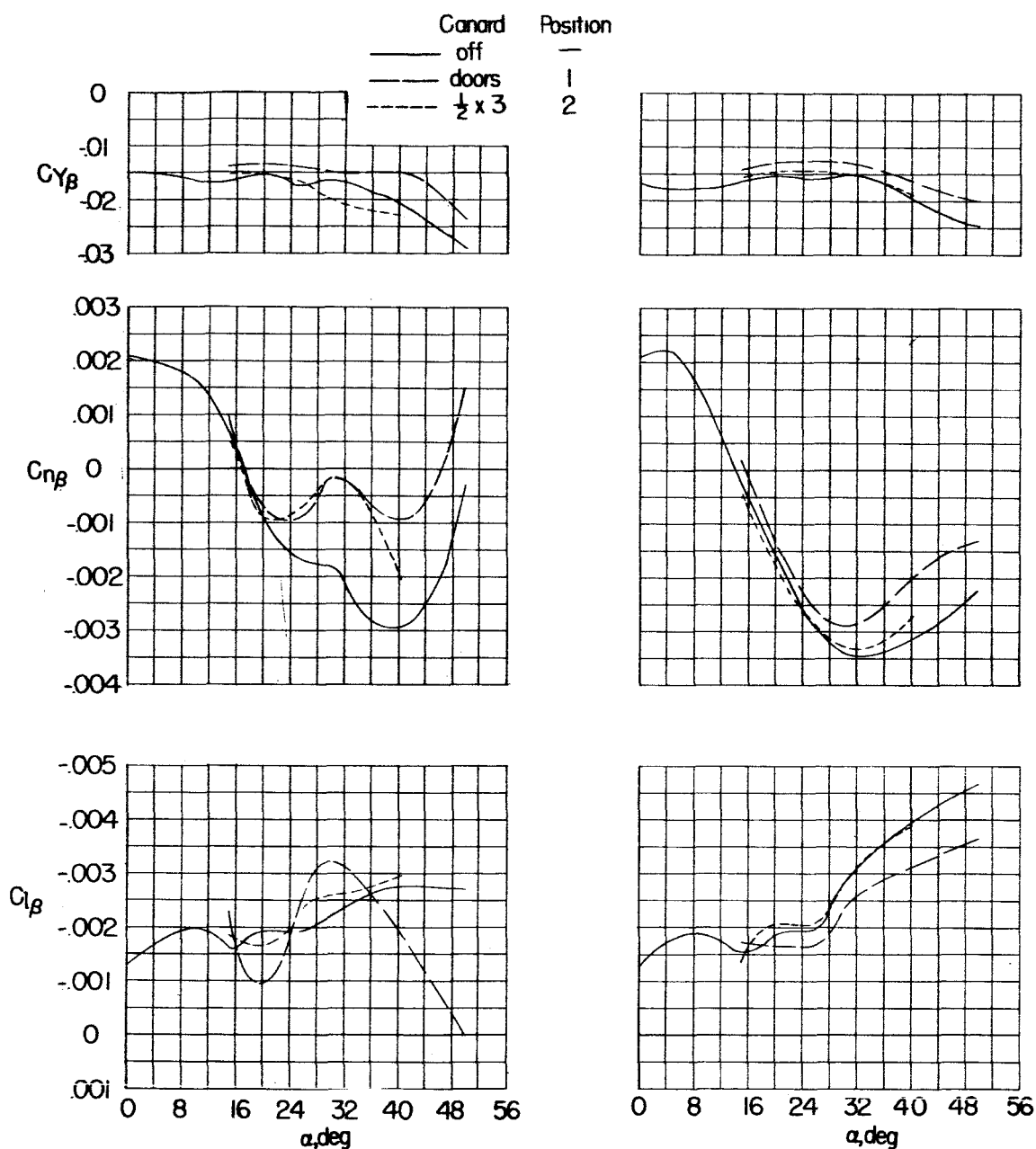
(a) $\beta = \pm 5^\circ$.(b) $\beta = \pm 20^\circ$.

Figure 10.- Effect of canard surfaces on the variation of static side-slip derivatives with angle of attack.

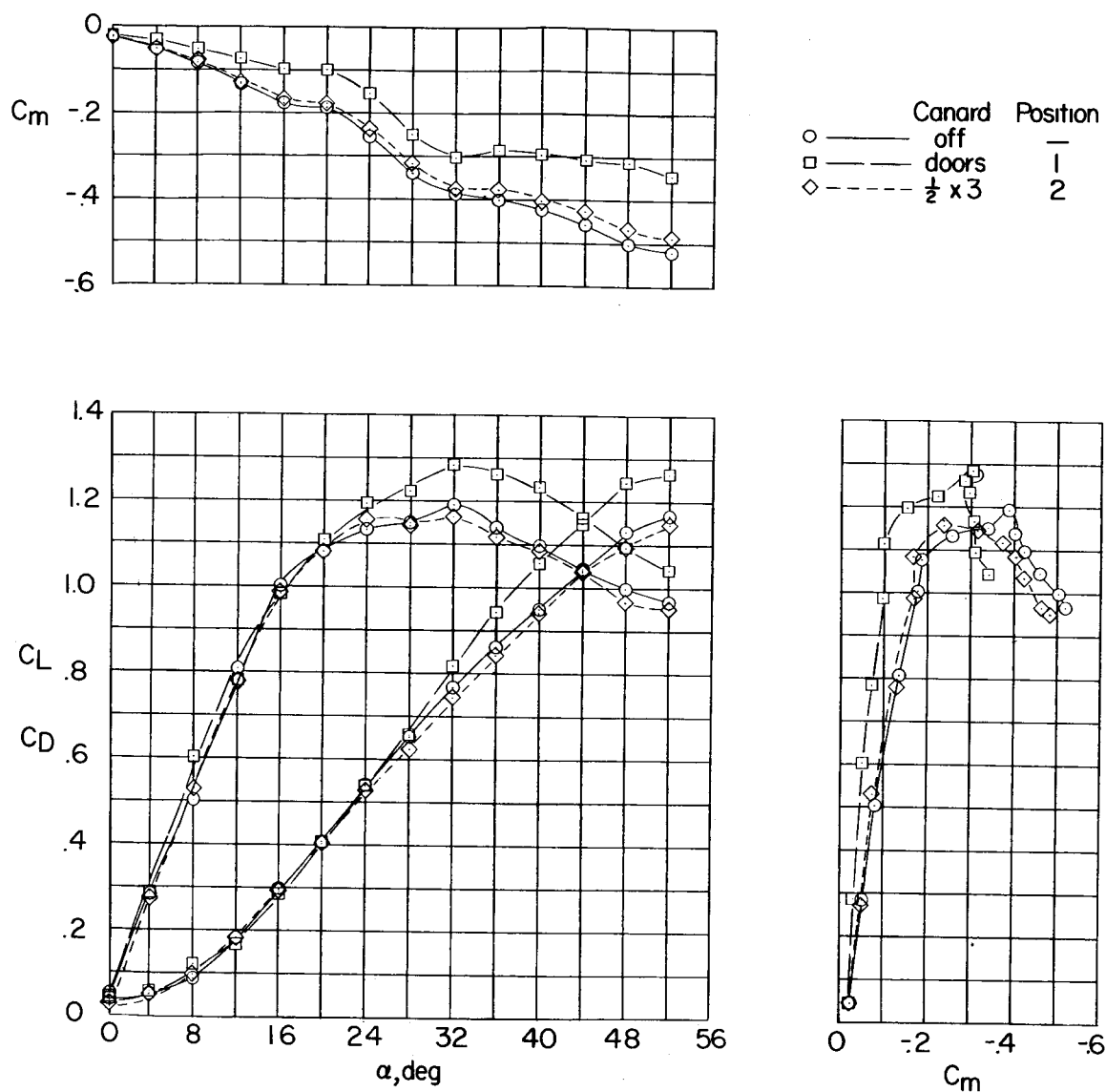


Figure 11.- Longitudinal characteristics of the model. $\beta = 0^\circ$.